8

Nexuses, sphalerons, and fractional topological charge

8.1 Introduction to nexuses and junctions

So far, it may appear that center vortices are embedded Abelian objects. But center vortices can be extended to non-Abelian objects in several ways. We describe two: the first we call junctions, representing the merging and branching of vortex lines (or sheets, in $d = 4$) without the necessity of monopole-like objects called nexuses; the second are nexuses themselves [1, 2, 3, 4], which are modifications of 't Hooft–Polyakov monopoles but with their magnetic flux bundled into tubes that are parts of center vortices. The most interesting property of nexuses is that, along with center vortices, they admit the formation of quantum lumps of nonintegral topological charge [5, 6, 7, 8, 9, 10].[1] Nexuses do not change the picture of confinement given in this book in any material way, although this is not completely obvious. But they enter in a crucial way into a reinterpretation of Polyakov's [12] discussion of confinement in the $d = 3$ Georgi–Glashow model, as we indicate at the end of this section [2, 13].

Note that we continue to use the notation of Chapter 7. All sections are in Euclidean space, except for Section 8.3.2, which is in Minkowski space.

8.1.1 Junctions

Junctions are thick points ($d = 3$) or lines ($d = 4$) where a vortex can branch into other vortices [14, 15]. It is easy to draw them in $d = 3$, where they look like vacuum Feynman graphs. Figure 8.1 shows a simple example with four junctions in $SU(3)$, where three lines meet at each junction (up to N lines can meet at an $SU(N)$ junction, each associated with a distinct flux matrix Q_j).

---

[1] In $SU(2)$, sphalerons (see Section 8.3) can carry half-integral topological charge [11] as lines that form when an ordinary instanton is split in half and the halves are pulled apart.
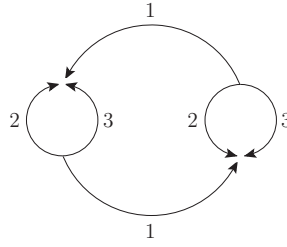
Figure 8.1. A junction and an antijunction in $SU(3)$. The numbers labeling the lines are the values of the index i in the flux matrix Q_i of each vortex line.

Suppose that one of the loops with lines labeled 2 and 3 meets the line labeled 1 at the origin 0. In the neighborhood of the origin, the junction term of the gauge potential is

$$\mathcal{A}_i(x) = \frac{2\pi}{i}\epsilon_{ijk}\partial_j \sum_{a=1}^{3} \int_0 dz(a)_k \, Q_a \{\Delta_M[z(a) - x] - \Delta_0[z(a) - x]\}, \quad (8.1)$$

where the Q_a are the three $k = 1$ matrices of $SU(3)$ discussed earlier.[2] Because $\sum^3 Q_j = 0$, the objection to open vortex lines, raised in Section 7.4.2, no longer applies; the would-be monopole charge, which is the sum of the Q_i, vanishes. For $N > 3$, there are configurations where some of the lines have higher flux: a k-vortex arises from associating a sum $Q_1 + Q_2 + \cdots$ with a single line integral.[3] Because of this feature, junction lines are not topologically stable, but they can be *entropically* stable because the total configurational entropy of two or more junction lines is greater than the entropy of a fewer number. Whether they actually are entropically stable depends on a comparison of action and entropy, which we do not attempt here.

Every junction has an action above and beyond the action per length of the vortices to which it is attached. Generally, this action depends on the geometry of the junction (e.g., it vanishes if lines 2 and 3 of Figure 8.1 are collapsed into one). The case in which the three junction lines meet at right angles has the $d = 3$ value $2\pi m/g^2$ [1].

8.1.2 Nexuses, magnetic charge, and topological charge

In NAGTs where all gluons have mass (not necessarily equal, so we contemplate Higgs–Kibble effects here, as in the Georgi–Glashow model), the radially

---

[2] Note that the lines are oriented, and they either all go in or all go out of the junction at the origin. We need not specify the upper limits of integration, which are irrelevant to the present discussion.
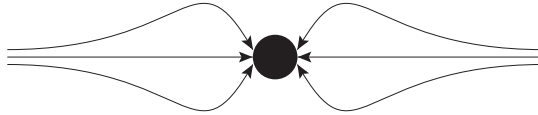[3] For $SU(3)$, there is no nontrivial junction with $k > 1$.

Figure 8.2. An $SU(2)$ nexus, showing two tubes of field lines.

symmetric long-range magnetic field of the 't Hooft–Polyakov monopole is squeezed into two or more flux tubes, as shown in Figure 8.2. These flux tubes, which must close either at infinity or on an antinexus, have magnetic flux quantized in the center of the gauge group, just as for center vortices, and for exactly the same reason: gluon wave functions must be single valued on transport around one of the tubes. In fact, these tubes are nothing but pieces of center vortices, divided up by closed nexus and antinexus world lines. So in the simplest case of two flux tubes, each tube has the same Π_1 homotopy exemplified in Eq. (7.40), except that each tube has a different representative of the set of matrices $Q_j(k)$. It will turn out that the total flux of the two tubes together is just that of a 't Hooft–Polyakov monopole for every $SU(N)$.

The field lines from the nexus shown in Figure 8.2 must close, which requires the presence of an antinexus. So a simple $d = 4$ case of a center vortex with nexuses is a torus, with a nexus world line and an antinexus world line (nonintersecting) wrapped around it. These world lines effectively divide the center vortex into regions of different orientation; the center vortex as a whole is nonorientable. This, it turns out, is crucial to the formation of topological charge.

Let us reduce the topological charge to its topological essentials by saving only the long-range pure-gauge parts of vortices and nexuses, which have singular fields on their Dirac surfaces and lines. There are several ways to think of this topological charge:

1. It is formed when a nexus world line links to a center-vortex surface [7, 8, 9, 10, 16].
2. It is measured by the usual $\int \mathcal{G}\tilde{\mathcal{G}}$ topological charge integral, which can be interpreted both as the signed intersection number of nonorientable surfaces and as the vortex-nexus linking number [7, 8, 9, 10, 16]. A special case of this occurs when vortices carry twist or writhe [5, 6, 7, 8, 9, 10, 16].
3. It can be interpreted in terms of a monopole magnetic charge, as defined by a standard integral of the type $\int \vec{\mathcal{B}} \cdot d\vec{S}$ over a closed two-sphere [17].

In all cases, the topological charge is divided into nonintegral parts. Generically, two closed surfaces intersect in an even number of points[4]; in this case, the topological

---

[4] The points actually have an extension of size $\sim 1/m$ if we save short-range parts of the gauge fields.

charge associated with each such point is quantized in units of $1/N$, but the total charge is integral if the surfaces are compact. Later we will see that self-intersection effects from twist and writhe [18] can lead to topological charge that is nonintegral but otherwise of any size.

Standard textbooks say that topological charge is manifested through instantons, which are compact lumps of integrally quantized topological charge. Actually, there is no reason for any given compact lump of topological charge to have any particular value, integral or otherwise. It may (and does) happen that the compact lumps carry nonintegral charge, but in such a way that the *global* topological charge, integrated over all Euclidean four-space, is an integer. This integrality result, however, is not automatic but depends on the assumption of *compactification* of the three-space bounding $d = 4$ space at infinity to a three-sphere S^3. The gauge potentials carrying topological charge now involve a map from the three-sphere to these potentials. The gauge group $SU(N)$ is either $SU(2)$ or has $SU(2)$ as a proper subgroup, and $SU(2)$ is topologically equivalent to S^3. So these maps are just maps of S^3 to S^3. Another way of speaking of these maps is through the homotopy

$$\Pi_3(SU(2)) \sim Z. \tag{8.2}$$

This one is easy; it just says that all maps of S^3 onto itself consist of an integral number of wrappings of one sphere onto another.[5] So in a $d = 4$ space whose boundary can be compactified, the *total* topological charge has to be an integer. However, this does not require that compact lumps of topological charge have integral charge, as instantons do, and we have already seen that nonintegral lumps do exist in the forms of nexus-vortex intersections and related objects. Global compactification simply requires that the sum of all the charges, integral or nonintegral, be an integer.

8.2　Nexuses in $SU(N)$

8.2.1　The SU(2) nexus

The first step [1, 16] is to find the gauge representative of an $SU(2)$ nexus in $d = 3$. There are infinitely many choices; a simple one is

$$U = \exp\left[\frac{i}{2}\phi\vec{\tau} \cdot \widehat{r}\right], \tag{8.3}$$

where the $\vec{\tau}$ are Pauli matrices and other symbols have their usual meaning. Later we will see that the generalization to $SU(N)$ is quite straightforward. From this

---

[5] Because any $SU(N)$ has $SU(2)$ as a subgroup, it turns out that $\Pi_3(SU(N)) \simeq Z$ for all N, so our arguments about integrality of topological charge apply for all gauge groups.

gauge representative, we can find the Dirac-string fields; they are

$$\frac{1}{2}\epsilon_{ijk}\mathcal{G}_{ij} = -\left(\frac{\tau_3}{2i}\right)\widehat{z}_i\epsilon(z)2\pi\,\delta(x)\delta(y). \tag{8.4}$$

These differ crucially from the corresponding Abelian expression by the factor $\epsilon(z)$, showing that the field lines reverse direction at the origin, which is where this Dirac nexus sits.

This Dirac nexus is beginning to show features like those of the nexus in Figure 8.2. To find the appropriate kinematics, form the gauge representative $\mathcal{A}_i \to U\partial_i U^{-1}$, and by inspection, choose for the full potential

$$\mathcal{A}_j = \frac{\epsilon_{jak}}{2i}\tau_a\widehat{r}_k[F - 1 + G\cos\phi] + \frac{1}{2i}(\tau_i - \widehat{r}_i\tau\cdot\widehat{r})G\sin\phi + \widehat{\phi}_j\frac{\tau\cdot\widehat{r}}{2i}B_1, \tag{8.5}$$

with

$$F = F(\rho, z); \qquad G = G(\rho, z); \qquad B_1 = B_1(\rho). \tag{8.6}$$

The function B_1 carries the thick flux tube of the center vortex (but with oppositely directed flux on the two halves of the z-axis), and so this kinematics describes a compound of a thick center-vortex flux tube and the nearly pointlike core of the nexus, just as in Eq. (7.21):

$$B_1 = \frac{1}{\rho} - mK_1(m\rho). \tag{8.7}$$

Choose boundary conditions to make the gauge potential approach the pure gauge based on the gauge representative of Eq. (8.3):

$$\rho, z \to \infty: \quad F \to 0, \ G \to -1 \tag{8.8}$$

$$\rho, z \to 0: \quad F \to +1, \ G \to 0.$$

There is no analytic solution to these coupled, nonlinear, partial differential equations, and no one has yet solved them numerically. However, there is a simple and useful variational approximation [1] using trial functions with a single variational parameter λ:

$$F = \frac{\lambda^2}{\lambda^2 + r^2}; \qquad G = -\frac{\rho r}{\lambda^2 + \rho r}. \tag{8.9}$$

These obey the correct boundary conditions. To find the nexus energy, calculate the entire Hamiltonian with these functions and subtract from it the energy of the pure vortex. One finds, after carrying out the usual variational steps, a nexus energy $3.22(4\pi m)/g^2$.

8.2.2 The SU(N) nexus

All this generalizes to $SU(N)$, although (just as with junctions) there are many new geometries. Note that a nexus, as the boundary between two regions of a vortex with differing field strengths, cannot have its tubes of chromomagnetic field separated into two bundles arbitrarily. It is essential that a center vortex decorated with a nexus give rise to precisely the same element of the center group, as found by transporting the gauge representative around a closed curve linking with the vortex for each flux tube. So for any nexus that has exactly two flux tubes, as in Figure 8.2, if one of the tubes carries flux matrix Q_1, e.g., then the other must carry another Q_j (and similarly for higher-flux matrices).

An elementary calculation shows that for any two choices of Q_k, their difference $Q_i - Q_j$ is a Pauli matrix τ_3 for an embedded $SU(2)$. This means that all entries are zero, except for one $+1$ (in the jth position along the diagonal) and one -1 (in the ith position). So we can write, e.g.,

$$Q_1 = -\frac{1}{2}\tau_3 + R(12), \qquad Q_2 = \frac{1}{2}\tau_3 + R(12),$$

$$R(12) = \mathrm{diag}\left(-\frac{1}{2} + \frac{1}{N}, -\frac{1}{2} + \frac{1}{N}, \frac{1}{N}, \ldots\right). \tag{8.10}$$

The matrix R_{12} commutes with the generators of the embedded $SU(2)$. Now it is elementary to find a gauge representative of a two-tube nexus:

$$U = \mathrm{e}^{(i\phi\tau\cdot\hat{r}/2)}\mathrm{e}^{i\phi R(12)}, \tag{8.11}$$

where, of course, the Pauli matrices are in the embedded $SU(2)$. The magnetic charge of the nexus can be identified with the eigenvalues of the embedded τ_3, which are ± 1, as would be required for a 't Hooft–Polyakov monopole.

8.2.3 Nexus magnetic charge

How do we detect the nexus magnetic charge and relate it to topological charge? Because there is a strong connection between the nexus and the 't Hooft–Polyakov monopole, the procedure [17] somewhat resembles that for the 't Hooft–Polyakov monopole. The main difference is that there is no Higgs–Kibble field for the nexus in a QCD-like theory. In the 't Hooft–Polyakov monopole, the presence of this Higgs–Kibble field in the adjoint of $SU(2)$ breaks the gauge symmetry to $SU(2)/U(1)$, a space homotopic to the two-sphere S^2, and the surviving long-range magnetic field can be identified with, say, the 3 direction in group space. After a suitable projection onto this unbroken $U(1)$ subspace, the magnetic charge of the
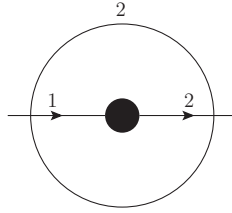
Figure 8.3. The inner black dot represents a nexus that we label A, and the lines represent its associated flux tubes with fluxes described by $Q_{1,2}$. The outer circle represents the plain vortex surface B with flux described by Q_2.

't Hooft–Polyakov monopole is measured through the integral

$$\int_{\Gamma} d\vec{S} \cdot \vec{\mathcal{B}} = Q_{\text{mag}},\tag{8.12}$$

where Γ is an arbitrary closed surface surrounding the monopole; the integral yields an integral magnetic charge Q_{mag}. This corresponds to the homotopy that maps this broken gauge group onto the two-sphere:

$$\Pi_2(SU(2)/U(1)) = \Pi_2(S^2) = Z,\tag{8.13}$$

where Z is the group of integers.

There is a sense in which nexuses also display this homotopy, although this is suspicious because there is no symmetry breaking for the nexus for QCD-like theories, and the homotopy $\Pi_2(G)$ is trivial for every non-Abelian gauge group G. What in fact happens is that nexuses really display *topological charge* and the homotopy above [17] is simply a disguised form of the usual topological charge integral:

$$Q_{\text{topo}} = -\frac{1}{16\pi^2} \int d^4x \, \text{Tr} \, \mathcal{G}_{\mu\nu}\widetilde{\mathcal{G}}_{\mu\nu}.\tag{8.14}$$

We evaluate this integral for the generic intersection of the static nexus already displayed with Dirac fields $\mathcal{G}_{\mu\nu}^{(A)}$ (see Eq. (8.4)) and a plain center vortex that we call (B), as in Figure 8.3. The static nexus is the horizontal line with incoming flux matrix Q_1 on the left and $-Q_2$ on the right. The center vortex surface (B) is a closed surface with the topology of S^2 characterized by the matrix Q_2. The vortex and the nexus intersect at two points, and these are where the topological charge density is located. The topological charge of the overlap between (A) and (B) is

$$Q_{\text{topo}} = -\frac{1}{8\pi^2} \int d^4x \, \text{Tr} \, \widetilde{\mathcal{G}}_{\mu\nu}^{(B)}\mathcal{G}_{\mu\nu}^{(A)} = \frac{1}{4\pi i} \int d\sigma_{\mu\nu} \, \text{Tr} \, Q_2\mathcal{G}_{\mu\nu}^{(A)},\tag{8.15}$$

where in the second equality, we replaced $\tilde{\mathcal{G}}_{\mu\nu}^{(B)}$ by its Dirac-surface form. For $SU(2)$, there are only two Q-matrices: $Q_1 = -Q_2 = \tau_3/2$. Clearly, this second equality is precisely the magnetic charge integral Q_{mag}, which we now see is equal to Q_{topo}; both are equal to unity.

For general $SU(N)$, give nexus (A) the Q-matrices Q_a, Q_c, and give the vortex (B) the Q-matrix Q_b. Now the trace factor is

$$\text{Tr}\, Q_b\,(Q_a - Q_c) = \delta_{ab} - \delta_{cb}. \tag{8.16}$$

This, of course, has only the integral values $0, \pm 1$, vanishing if b is not equal to either a or c. The topological charge depends very much on the surface surrounding the nexus, unlike the purely artificial surface used to define the magnetic charge of a 't Hooft–Polyakov monopole. As advertised, the total topological charge is integral, with a fractional charge of $\text{Tr}\, Q_b Q_a = \delta_{ab} - (1/N)$ at the crossing of flux line a with the vortex surface. All this can be generalized to more complicated vortices and nexuses, but we will not do that here.

8.2.4 Topological charge as an intersection number for nonorientable vortex surfaces

Here we display the intersection number form of Q_{topo} [7, 8, 9, 10, 16]. Start with the vortex field strength in the Dirac-surface limit:

$$\mathcal{G}_{\mu\nu}^A(x) = \frac{2\pi Q_A}{i} \int d\tilde{\sigma}_{\mu\nu}^A(z)\, \delta(x - z(A)), \tag{8.17}$$

where Q_A is one of the flux matrices Q and $d\tilde{\sigma}_{\mu\nu}^A(z)$ is the dual surface element for the surface A characteristic of the vortex. The standard topological charge of Eq. (8.14) is, in terms of the sum of vortex field strengths,

$$Q_{\text{topo}} = \sum_{A,B} \text{Tr}(Q_A Q_B) I(A, B), \tag{8.18}$$

where $I(A, B)$ is an *intersection number*:

$$I(A, B) = \epsilon_{\mu\nu\alpha\beta} \int \frac{1}{2} d\sigma_{\mu\nu}^A \frac{1}{2} d\sigma_{\alpha\beta}^B\, \delta(z(A) - x(B)). \tag{8.19}$$

The intersection number is ± 1 for every transverse intersection of a point on surface A with a point on surface B (transverse means that the normals to the surfaces at the point of intersection span Euclidean four-space).

We are on the road to getting lumps of fractional topological charge localized at the intersection points because the trace factor $\text{Tr}(Q_A Q_B)$ always has a denominator of N for $SU(N)$. Unfortunately, at this stage of the game, we always get zero
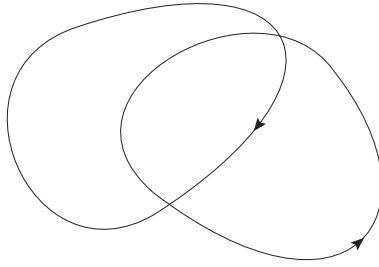
Figure 8.4. Two closed oriented lines in $d = 2$ have a total intersection number of zero because the two intersections have opposite orientation and cancel.
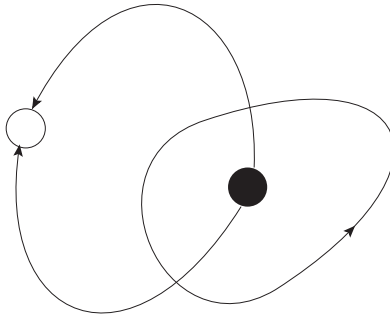

Figure 8.5. Two closed lines in $d = 2$, one with an $SU(2)$ nexus-antinexus pair. They have a total intersection number of 1 because the two intersections have the same orientation.

from Eq. (8.18) [7, 8, 9, 10, 16, 17]. The reason is that when two *closed oriented* surfaces intersect, the total intersection number is zero. One can see this from the corresponding geometry in two dimensions, as shown in Figure 8.4. We will give a formal proof that the total intersection number is zero in $d = 4$ very shortly.

For any pair of ordinary vortices, we can factor out the trace factor in Eq. (8.18), and then the resulting charge is zero. So intersections do not seem very promising for generating topological charge. We can fix the problem by remembering nexuses that in effect change the Q matrices, while preserving the group-center element associated with a vortex as one moves around a given vortex surface. The simplest case to illustrate is $SU(2)$, where a nexus simply changes the orientation of the chromomagnetic flux. Figure 8.5 shows two intersecting, two-dimensional closed curves, but this time, the one on the left has a nexus and an antinexus, reversing the orientation at each. The plain curve, on the right, encloses (is linked to) the nexus, and because the orientation reverses on passing the nexus, the intersection numbers are $+1$ at both intersections. The Q-trace is $1/2$, and now the topological charge is

$1/2 + 1/2 = 1$. The topological charge is still localized at the intersection points and is fractional at these points, but the total topological charge is unity.

The same thing – appearance of lumps of topological charge quantized in units of $1/N$, with integral total charge – happens in $d = 4$ and for any $SU(N)$ [5, 6, 7, 8, 9, 10, 16, 17]. Look at the simplest case, where a single nexus world line on one vortex is linked to a closed vortex with no nexuses. Nexus world lines that are unlinked contribute nothing and are omitted. With this understanding, write the dual field strength of vortex A with nexuses as a sum:

$$\widetilde{\mathcal{G}}^A_{\mu\nu}(x) = \frac{2\pi Q_a}{i} \int_{S_a} d\sigma_{\mu\nu}\, \delta(x - z(\sigma)) + \frac{2\pi Q_b}{i} \int_{S_b} d\sigma_{\mu\nu}\, \delta(x - z(\sigma)), \quad (8.20)$$

where S_a is a surface bounded by the closed nexus world line Γ on one side, and S_b is a surface bounded by the same world line on the other side. These boundaries have opposite orientation, in the sense that

$$\partial S_a = \Gamma \qquad \partial S_b = -\Gamma. \tag{8.21}$$

Equation (8.20) is not literally correct because terms that exhibit the corresponding antinexus world line, and possibly other nexuses and antinexuses, are omitted. However, they are irrelevant to the topological charge if they are not linked to the surface of the second vortex. This equation has another flaw: taken literally, it violates the Bianchi identities. This is because there really is no mathematically accurate way of modeling a nexus as an Abelian object; it is essentially non-Abelian. One overcomes this Bianchi identity problem by smoothing the transition from Q_a to Q_b over a region of size $\sim 1/m$, as in the nexus; this smoothing has no effect on topological properties coming from long-range effects.

Let $\mathcal{A}^C_\mu(x)$ be the Dirac-singular part of the gauge potential of a second vortex with no nexuses. Its Dirac gauge potential is an integral over a closed surface S_c:

$$\mathcal{A}^C_\mu(x) = -\frac{2\pi Q_c}{i} \epsilon_{\mu\nu\alpha\beta} \oint_{S_c} \frac{1}{2} d\sigma'_{\alpha\beta}\, \Delta_0(x - y(\sigma')). \tag{8.22}$$

The topological charge is expressible as a linking between the vortex and the nexus world line, completely analogous to the linking of a vortex and a Wilson loop responsible for confinement. The Gauss formula for linking vortex surface S_c and the closed nexus world line Γ is familiar from confinement:

$$Lk = \oint_\Gamma dz_\mu \epsilon_{\mu\nu\alpha\beta} \oint_{S_c} \frac{1}{2} d\sigma'_{\alpha\beta}\, \partial_\nu \Delta_0(z - y(\sigma')). \tag{8.23}$$
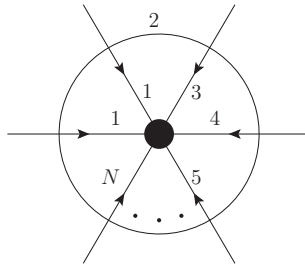
Figure 8.6. An $SU(N)$ nexus split into N lines. The circle labeled 2 schematically represents the plain vortex (B) of the text, and the vortex flux lines emerge from the nexus (A). The intersections of the lines and the circle are points of topological charge density.

Next, we show that the topological charge is essentially this link number by applying Stokes's theorem. Consider the expression

$$Q_{\text{topo}} = \frac{1}{2\pi i} \oint_{\Gamma} dx_{\mu} \, \text{Tr} \left[(Q_a - Q_b) A_{\mu}^{C}(x) \right] \tag{8.24}$$

for the topological charge. Using Stokes's theorem on Eq. (8.24) yields an expression that is easily converted into the fundamental topological charge integral of Eq. (8.14), evaluated with the field strengths from Eq. (8.20) and the curl of Eq. (8.22). The minus sign in the trace factor comes from the opposite orientations, as given in Eq. (8.21).

We can also conclude from Eq. (8.24) that the total intersection number of closed oriented surfaces is zero by replacing the individual trace factors $\text{Tr} \, Q_a Q_c$ and $\text{Tr} \, Q_b Q_c$ by unity.

We have earlier seen how to divide topological charge into parts $1 - (1/N)$ and $1/N$. Is it possible to divide this topological charge further into N constituents, each of charge $1/N$? The answer is yes. In the center vortex of Figure 8.3, decompose the flux matrix Q_2 on the right-hand side (rhs) of the nexus as

$$Q_2 = -Q_1 - Q_3 \cdots - Q_N, \tag{8.25}$$

and associate a flux tube with each of the terms in this equation, as shown in Figure 8.6.

Each intersection of a line coming from the nexus (A) with the circle (B) is a point of topological charge $1/N$, with the sum being unity, as before. Is it probable that an elementary nexus would split into N lines, as shown? Not if action alone were the only consideration because the N lines each have an action per unit area the same as that of the two lines of an elementary nexus. But as we have learned, entropy is equally important, so this N-line splitting should not be less probable than a 2-line nexus.
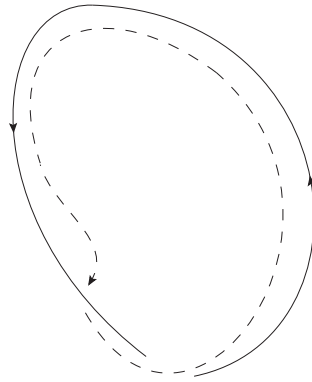
Figure 8.7. A curve turned into a ribbon by adding the curve of the dotted line.

How might one see the effect of fractional topological charge, especially because topological charge is integrally quantized globally? Perhaps the most important way is to study the topological susceptibility χ, which is quadratic in Q_{topo}. This is defined as $\chi = \langle Q_{\text{topo}}^2 \rangle / V_4$, where V_4 is the volume of space-time. Witten [19] and Veneziano [20] have given a large-N formula relating the η' mass to χ, which suggests that the vacuum energy as a function of the θ-angle depends not on θ but on θ/N, as topological charge fractionation would give. This is discussed further in [16].

But topological charge fractionation into units of $1/N$ is, unfortunately, not the whole story. Center vortices need not intersect at points to generate nonintegral topological charge; they can do so by twist and writhe [5, 6, 7, 8, 9, 10, 16, 17].

Twist and writhe   An ordinary two-dimensional ribbon can link to itself (in $d = 3$) by twist and writhe, which means by deformations such that the two edges of the ribbon would be linked (knotted) if the rest of the ribbon were missing.[6] Twist and writhe contribute to the Chern–Simons number in somewhat the same way that intersections contribute to the topological charge [5, 6, 7, 8, 9, 10]; that is, for a vortex with twist, writhe, or both, the integral for N_{cs} in Eq. (8.31) is nonvanishing, and this integral need not be integral or a multiple of $1/N$.

Intuitively, twist comes from forming this ribbon from a long, open paper strip then twisting one end a certain number of times before closing the strip by joining one end to the other. (A half twist leads to a nonorientable Möbius strip not considered here.) For a mathematical curve, twist and writhe need further definition, which can be done by supplying the curve with an infinitesimally close partner, as shown in Figure 8.7. The combination forms a ribbon whose twist and writhe are well defined but not unique (they depend on the partner curve).

---

[6] See Kaufmann [18] for general properties of knots and related subjects.
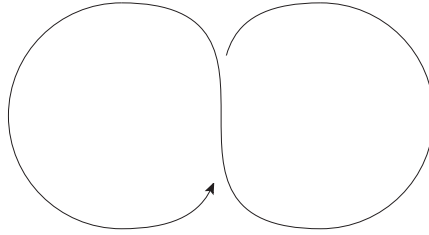
Figure 8.8. A $d = 3$ projection of a center vortex with writhe.

Writhe seems intuitively to be different from twist, but it is not. Figure 8.8 shows a closed curve with writhe. Playing with actual paper ribbons will show that twist and writhe are interconvertible without tearing the paper.

Topological charge can be generated from twist and writhe only if there is a difference in the Chern–Simons number at two boundaries that we can identify as referring to (Euclidean) times of $\pm\infty$ so that if the vortex is to change its Chern–Simons number, it must reconnect by crossing itself. This crossing may be essentially Abelian and easily envisaged by imagining a motion picture of a closed loop crossing itself, or it can be essentially non-Abelian and call for a deeper level of visualization.

Consider, then, the closed Dirac string of a $d = 3$ vortex. There is a famous theorem of such $d = 3$ knotted curves,

$$Lk = Tw + Wr, \tag{8.26}$$

where Lk, a topological number and an integer, is the self-linking number, and the terms on the right, neither of which is an integer or of topological character, are the twist Tw and writhe Wr, respectively. The integral that defines Lk is just the one used earlier (see Eq. (7.41)) for the linkage of two distinct curves but with only one curve in it:

$$Lk = \oint_\Gamma dx_i \oint_\Gamma dx'_j \epsilon_{ijk} \partial_k \Delta_0(x - x'). \tag{8.27}$$

With just one curve Γ, it is inevitable that the points where $x = x'$ are possibly singular. Some form of regulator is needed. The standard one is *ribbon framing*, as in Figure 8.7. The original curve is turned into a ribbon by adding a second curve Γ' infinitesimally separated from Γ and not intersecting it; the self-link number is defined as the Gauss link integral for these two nonintersecting curves. So Γ' is the first curve displaced by an infinitesimal amount:

$$\Gamma' : \qquad x'_i(s) = x_i(s) + \epsilon n_i(s), \tag{8.28}$$

where ϵ is infinitesimal and $n_i(s)$ is a unit-vector field. The self-link number is defined as the mutual link number of Γ and Γ'. This is, to be sure, an integer and a topological invariant, but it depends on this new unit-vector field.

This ribbon framing would not make sense for real-world center vortices because we have no good way of defining the framing, and even the topologically invariant self-link is only defined modulo integers that depend on the framing. But real-world center vortices have a finite thickness, as we know. This thickness removes all ambiguity from the limiting process of defining self-linkage. The idea [5] is to write the Chern–Simons number, which is the same as the linking number, for a vortex using both the massive and the massless propagators that occur in the vortex wave function. It then turns out that the Chern–Simons number for a plain unit-flux vortex becomes

$$N_{\mathrm{CS}} = \mathrm{Tr}\, Q_i^2 \oint_\Gamma \mathrm{d}x_i \oint_\Gamma \mathrm{d}x_j'\, \epsilon_{ijk} \partial_k \Delta_0(x - x') F(M|x_i - x_i'|), \qquad (8.29)$$

where

$$F(u) = \frac{1}{2} \int_0^u \mathrm{d}v\, v^2 \mathrm{e}^{-v}. \qquad (8.30)$$

For small u, $F(u) \sim u^3$, and this is more than enough to cancel the singularities at $x_i = x_i'$ in the rest of the integrand in Eq. (8.29). Since $F(\infty) = 1$, vortex segments that are far apart contribute as usual to the Chern–Simons number, and nothing is changed.

The topological charge contained between two time slices is the difference between two Chern–Simons numbers. For a gauge potential on a fixed-time slice, this number is

$$N_{\mathrm{CS}} = -\frac{1}{8\pi^2} \int \mathrm{d}^3x\, \epsilon_{ijk} \mathrm{Tr}\left(\mathcal{A}_i \partial_j \mathcal{A}_k + \frac{2}{3}\mathcal{A}_i \mathcal{A}_j \mathcal{A}_k\right). \qquad (8.31)$$

This number is not gauge invariant; under the gauge transformation

$$\mathcal{A}_i \to U\mathcal{A}_i U^{-1} + U\partial_i U^{-1}, \qquad (8.32)$$

we find

$$N_{\mathrm{CS}} \to N_{\mathrm{CS}} + \frac{1}{8\pi^2} \int \mathrm{d}^3x\, \epsilon_{ijk} \mathrm{Tr}\left[\frac{1}{3}U^{-1}\partial_i U U^{-1}\partial_j U U^{-1}\partial_k U - \partial_i(\mathcal{A}_j U^{-1}\partial_k U)\right]. \qquad (8.33)$$

If the original gauge potential is zero, so that we are calculating the Chern–Simons number of a pure gauge transformation, the integral in Eq. (8.33) is supposed to be an integer, as prescribed by the homotopy of Eq. (8.2). However, this requires

an extra assumption: that the three-space over which one integrates the Chern–Simons density is *compact*, which means that the gauge $U(\vec{x})$ approaches a constant independent of direction as $r \to \infty$. There seems to be no elementary physical reason for assuming compactness, and in Section 8.3, devoted to the sphaleron, we examine this assumption further (the sphaleron naturally has $N_{\text{CS}} = 1/2$, seemingly violating compactness).

Nexuses in the Georgi–Glashow model In a famous paper, Polyakov [12] explained confinement in the $d = 3$ Georgi–Glashow model as due to 't Hooft–Polyakov monopoles, with a long-range spherically symmetric magnetic field, thereby exemplifying dual superconductivity as a confining mechanism. (The Georgi–Glashow model is an $SO(3)$ NAGT coupled to a Higgs–Kibble field in the adjoint representation, which gives masses to two charged gauge bosons, leaving the third one, which we call the photon, massless.) In fact [2, 13], confinement in the Georgi–Glashow model is actually an example of center-vortex confinement with asymmetric nexuses, whose world lines lie in center-vortex sheets, as we have already shown for QCD-like gauge theories with no symmetry breaking. Polyakov works in the limit $v \gg g_3$, where v is the Higgs–Kibble VEV and g_3 is the gauge coupling. In this, the semiclassical limit, the 't Hooft–Polyakov monopole has a very large action. Because there must be a monopole condensate, Polyakov points out that a Meissner mass is induced for the photon, just as in ordinary superconductivity. This mass, however, is exponentially small in v/g_3 and is ignored by Polyakov, who then can claim that the semiclassical excitations of the gauge field are indeed 't Hooft–Polyakov monopoles. But as long as v is finite, the 't Hooft–Polyakov monopole becomes a nexus because its magnetic field can no longer be long range. The size of the nexus is exponentially large and, at distances scaled by other parameters of the theory, looks very much like a 't Hooft–Polyakov monopole. Nonetheless, as a matter of principle, for (fundamental representation) Wilson loops that are large compared to the nexus thickness, confinement is by the center vortices in which the nexus is embedded. This becomes clear [13] as the VEV v is reduced; at some point, when $v \le g_3$, the Higgs–Kibble mass of the charged gauge bosons, proportional to vg_3, is too small to avoid infrared instability, a dynamical gauge-boson mass of $\mathcal{O}(g_3^2)$ is induced, and the nexus (and center vortices) begin to look like the symmetrical ones of a QCD-like theory.

8.3 The QCD sphaleron

There are three gauge-field configurations known as sphalerons. Usually the word *sphaleron*[7] refers to a massive spherically symmetric $d = 3$ electroweak soliton

---

[7] Coined by Klinkhamer and Manton [21].

with a gauge-boson mass driven by a Higgs field [22]. The sphaleron's topological properties were first noted for electroweak theory by Manton [22], where it occurred as a classical saddlepoint on a noncontractible loop in the $d = 3 + 1$ configuration space of gauge potentials, describing the top of the tunneling barrier of minimum energy between vacua with topological charges differing by unity. There is another sphaleron in classical NAGTs corresponding to the saddlepoint at the top of the potential barrier tunneled through by instantons. This classical object is massless but has an arbitrary length scale set by the collective size coordinate of its associated instanton.

There is also a quantum sphaleron in QCD-like NAGTs [23] that differs from both of the preceding sphalerons while retaining the saddlepoint character; we call it the QCD sphaleron. The gauge-boson mass is dynamical, there is no Higgs–Kibble field, and there is no symmetry breaking. The QCD sphaleron has a fixed size determined by the gluon mass, and this size actually corresponds to an upper limit for the size of instantons and sphalerons. This sort of upper size limit is routinely seen in computer simulations in which instantons are identified and built into models [24] of the instanton liquid, where the size scale corresponds to a mass of 600 MeV. The QCD sphaleron may exist transiently as some sort of glue ball, and it also is a mediator between charge-changing events but not of the usual topological charge. Instead, the charge associated with the QCD sphaleron is that of the color-singlet axial current, giving the change in the flavor sum of chiralities.

Both the classical sphaleron and the QCD sphaleron can be embedded in Euclidean four-space ($d = 4$) or in Minkowski space ($d = 3 + 1$), and these embeddings will be the emphasis in the present chapter. (Chapter 9 discusses the sphaleron as a $d = 3$ object more fully.) In $d = 4$, the classical sphaleron is a cross section of an instanton that solves the classical field equations. In $d = 3 + 1$, there is no known embedding in a solution of the field equations, but one can find embeddings that have all the desired properties of an evolution of topological charge in Minkowski time t [25, 26] and define a corresponding Chern–Simons number $N_{cs}(t)$. By symmetry of the tunneling process from topological charge zero to charge unity, we should assign a Chern–Simons number or topological charge of $1/2$ to the sphaleron and describe the tunneling, in Minkowski time, as a smooth evolution of $N_{cs}(t)$ from 0 to 1, passing through $1/2$ at the top of the barrier. In the course of this smooth evolution, N_{cs} is clearly nonintegral because it gets contributions from gauge potentials that are not pure gauge with nonvanishing field strengths. Like the other solitons we discuss, the QCD sphaleron is fundamentally a $d = 3$ object but is unstable in isolation. After discussing this basic QCD sphaleron, we defer to Chapter 9 for further discussion of the QCD sphaleron as a pure $d = 3$ object and will show [27] that, considered purely as a $d = 3$ object, the $N_{cs} = 1/2$ sphaleron

is closely connected to the properties of knots or closed $d = 1$ strings, embedded in three dimensions, that are linked.

There are many potential physical applications of sphalerons, both in electroweak theory and in QCD. Some arise through the connection, via the anomaly, of topological charge and the divergence of a current. In electroweak theory, this current is the sum of the baryonic (B) and leptonic (L) current and leads to B + L violation. In QCD, the current with an anomalous divergence is the $U_A(1)$ current, and helicity conservation is violated. In both cases, the violations have a tunneling interpretation. Sphaleronic configurations are also important in estimating the (lack of) overlap at high energy between few-particle states and many-particle states; see the references in Chapter 9. It would take almost another book to detail such applications.

8.3.1 The QCD sphaleron as a $d = 3$ object

The ansatz for the gauge function U of the sphaleron is the well-known one for spherically symmetric solitons,

$$U = \exp\left[\frac{i}{2}\beta(r)\vec{\tau} \cdot \hat{r}\right], \tag{8.34}$$

differing from Eq. (8.3) of the nexus only in the choice of a rotation angle, which for the sphaleron is radially symmetric. Forming the pure-gauge representative $\mathcal{A}_i \to U\partial_i U^{-1}$, we infer the standard kinematics for spherically symmetric solitons:

$$\mathcal{A}_j = \frac{\epsilon_{jak}}{2i}\tau_a\hat{r}_k\left[\frac{\phi_1(r) - 1}{r}\right] - \frac{1}{2i}(\tau_j - \hat{r}_j\tau \cdot \hat{r})\left[\frac{\phi_2(r)}{r}\right] + \hat{r}_j\frac{\tau \cdot \hat{r}}{2i}H_1(r). \tag{8.35}$$

The boundary conditions are as follows:

$$\phi_1(\infty) = \cos\beta(\infty); \qquad \phi_2(\infty) = -\sin\beta(\infty); \qquad H_1 \to \left.\frac{d\beta}{dr}\right|_{r=\infty}. \tag{8.36}$$

For future reference (see Chapter 9), we note that the Chern-Simons number of U is

$$N_{CS}\{U\} = \frac{1}{2\pi}[\beta(\infty) - \beta(0)]. \tag{8.37}$$

The equations of motion have a finite-energy solution [23] for the special choice $\beta(r) = \pi$. There is no analytic solution, but there is an analytic approximation [11, 23] based on a variational approach that gives excellent agreement with numerical calculations. Use the trial functions

$$\phi_1(r) = \frac{a^2 - r^2}{a^2 + r^2}; \qquad \beta = \pi; \qquad \phi_2 = H_1 = 0, \tag{8.38}$$

where the length a is a variational parameter. Of course, the true $\phi_1 + 1$ vanishes exponentially as $r \to \infty$, but our trial wave function vanishes only like $1/r^2$. The variational mass turns out to be $5.44(4\pi m/g^2)$, which is within half a percent of the numerical answer, in which 5.44 is replaced by 5.41.[8]

One might think that if β is a half-integral multiple of π, the CS number is also a half-integral. But Eq. (8.37) shows that N_{CS} vanishes. Only when we embed this sphaleron in a $d = 3 + 1$ context will we find a Chern–Simons number of $1/2$. In any event, we can change the Chern–Simons number arbitrarily by making a spherical gauge transformation, although at the price of foregoing compactness.

As a solution of the spherical field equations, this $\beta = \pi$ sphaleron is an extremum, but it is a saddlepoint and therefore has a maximum for some parameters in a space orthogonal to a space in which the minimum lies (in our case, this space is just the space of the trial parameter a). For example, Ref. [11] exhibits trial functions yielding finite energy and having $\beta = \beta_0$ for any fixed angle β_0. Let ϕ_{1c} be the exact solution for the $\beta = \pi$ sphaleron, and define

$$\phi \equiv \phi_1 + \mathrm{i}\phi_2 = \frac{1}{2}(1 + \phi_{1c}) + \frac{1}{2}\mathrm{e}^{\mathrm{i}\beta_0}(1 - \phi_{1c}). \tag{8.39}$$

Also, take $H_1 = 0$. The new ϕ obeys the boundary conditions of Eq. (8.36) with $\beta = \beta_0$, and the associated gauge potential, constructed from $\phi - 1$, smoothly changes toward zero as $\beta_0 \to 0 \bmod 2\pi$. The trial mass function is

$$M_s(\beta_0) = \frac{1}{2}(1 - \cos\beta_0)M_s(\beta_0 = \pi), \tag{8.40}$$

where $M_s(\beta_0 = \pi)$ is the sphaleron mass. So there is a maximum at $\beta_0 = \pi$, and smoothly reducing β_0 to zero reduces the soliton to nothing.

8.3.2 Sphalerons in four-dimensional Minkowski space

There is a very simple but apparently accurate description [25, 26] of this minimum-height barrier that has only one dynamical degree of freedom, a simple scalar function of time called $\lambda(t)$. It nicely extends the trial function of Eq. (8.38) to time-dependent configurations. Bitar and Chang [25] suggested that the standard expressions for a classical instanton could be used in Minkowski space with the simple replacement of t by $\lambda(t)$ and the insertion of $\dot{\lambda}(t)$ at a particular place. These expressions, in terms of the spherically symmetric space components of Eq. (8.35), are

$$\phi_1 = \frac{\lambda^2 + a^2 - r^2}{\lambda^2 + a^2 + r^2}; \qquad \phi_2 = \frac{-2\lambda r}{\lambda^2 + a^2 + r^2}; \qquad H_1 = \frac{2\lambda}{\lambda^2 + a^2 + r^2}. \tag{8.41}$$

---

[8] Warning: in Cornwall [26], an incorrect value was used in place of 5.44. This paper also has several typos.

To this list, we add a time component of the gauge potential,

$$\mathcal{A}_0 \equiv \frac{1}{2i} \vec{\tau} \cdot \hat{x} \, H_2; \qquad H_2 = \frac{-2\dot{\lambda}}{\lambda^2 + a^2 + r^2}, \tag{8.42}$$

and take $\beta = 2 \arctan(r/\lambda)$. This choice for β is equivalent to making a spherical gauge transformation of the $d = 3$ spherical decomposition by an angle $\alpha = -\pi + 2 \arctan(r/\lambda)$ that carries λ as a parameter with no particular dynamical significance in $d = 3$.

If λ is replaced by t, these expressions are exactly those for an instanton in $d = 4$ of size a, which is arbitrary for the classical instanton. However, for the QCD sphaleron and its embedding, a has a different interpretation and is determined by the gluon mass m. As in Bitar and Chang, these embedding functions for the QCD sphaleron are used in Minkowski space, not Euclidean space. Of course, in Minkowski space, they are neither solutions of the equations of motion nor self-dual, but they are still useful because they represent the tunneling barrier itself quite accurately. Because λ in some sense is a replacement for time t, we require that λ be an odd function of t and monotone increasing in t, and we impose the conditions

$$\lambda(-\infty) = -\infty; \qquad \lambda(0) = 0; \qquad \lambda(+\infty) = \infty. \tag{8.43}$$

We have, consistent with the oddness in t of λ, $\dot{\lambda}(0) = 0$ at the time $t = 0$, representing the top of the barrier, where $\mathcal{A}_0$ vanishes according to our ansatz. Then, at $t = 0$ (i.e., $\lambda = 0$), the Bitar–Chang potentials reduce to the $d = 3$ trial function already used in Eq. (8.38) for the QCD sphaleron plus the specification $\beta = \pi$. The minimum QCD sphaleron barrier height at $t = 0$ is the sphaleron energy, and the saddlepoint nature of the sphaleron becomes evident because (see Eq. (8.44) below) as time increases, the energy decreases.

For the QCD sphaleron, we treat a as a variational parameter to be determined from the *massive* effective Hamiltonian. This Hamiltonian comes from inserting the full ansatz into the $d = 3 + 1$ action analogous to the $d = 4$ massive effective action S_{eff} and stripping off a time integral. It is not quite the same as the static Hamiltonian H_{eff} of Eq. (7.7) because there are contributions from the $\dot{\lambda}$ terms. The result [26] has the form

$$H_s = H_{\mathrm{eff}} + \frac{\dot{\lambda}^2}{2g^2} \mu(\lambda, a, m) - \frac{\lambda^2}{2g^2} \kappa(\lambda, a, m). \tag{8.44}$$

The first term on the right is the static (potential) energy H_{eff} at $\lambda = \dot{\lambda} = 0$, and μ, κ are positive integrals [26] over the Bitar–Chang potentials and fields. The sphaleron mass M_s is simply the extremal value of H_{eff}. At $t = 0$, extremalization

of H_{eff} leads to

$$a = \frac{\sqrt{3}}{2m}; \qquad M_s = \frac{4\sqrt{3\pi}\,m}{g^2}. \qquad (8.45)$$

The saddlepoint instability of the sphaleron is evident in the negative sign for the potential coefficient κ.

The Chern–Simons number varies smoothly with t from 0 at $t = -\infty$ to 1 at $t = +\infty$. The total topological charge has the expression

$$\begin{aligned}
Q_{\text{topo}} &= -\frac{1}{4\pi^2} \int d^4x \, \text{Tr} \, \vec{\mathcal{E}} \cdot \vec{\mathcal{B}} \\
&= \frac{24a^4}{\pi} \int_0^\infty dr \, r^2 \int_{-\infty}^\infty d\lambda \frac{1}{(\lambda^2 + r^2 + a^2)^4} = 1.
\end{aligned} \qquad (8.46)$$

The integral to the top of the barrier ($\lambda = 0$) gives topological charge 1/2, as expected, consistent with Eq. (8.37).

Now change variables from λ to a new variable angular $q(t) = f(\lambda(t))$, chosen so that the kinetic energy in the Hamiltonian has the simple form $\dot{q}^2/(2I)$, with a q-independent moment of inertia and with the angular properties $q(t = -\infty) = 0$, $q(t = +\infty) = 2\pi$. This has been done numerically [26], and the resulting potential looks very much like the pendulum potential $\sim 1 - \cos q$. The sphaleron is the static but unstable point $q = \pi$ with the pendulum standing on end.

The parameter β_0 introduced in Eq. (8.39) for the trial wave function, considered a function of time, is both (approximately) the phase variable q for the upside-down pendulum and the angle to be used in N_{cs} (see Eq. (8.37)).

8.4 Chiral symmetry breakdown, nexuses, and fractional topological charge

Chiral symmetry breaking (CSB) for quarks in QCD is closely related to confinement and (via the Atiyah–Singer theorem) a condensate of topological charge. Arguments were given long ago [28, 29, 30] that confinement was sufficient for CSB. These works were based on a variety of phenomenological models of confinement, not center vortices. Later, lattice simulations showed [31] that center vortices (and nexuses) were not only sufficient but also necessary for quark CSB: there was both confinement and CSB in the presence of center vortices, but when center vortices were removed from the simulation, not only did confinement disappear, but CSB disappeared also, as shown in Figure 8.9.

Moreover, simulations show that the CSB transition temperature, at which chiral symmetry is restored, is very close to the deconfinement transition temperature,
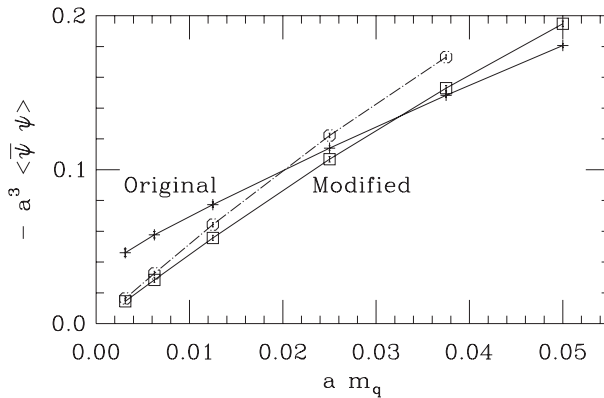
Figure 8.9. Graph of the quark condensate $\langle \bar{\psi} \psi \rangle$ versus quark mass m_q, showing CSB at $m_q = 0$ if center vortices are present (curve marked "Original") but not if they are removed (curve marked "Modified"). Reprinted with permission from P. de Forcrand and M. D'Elia, *Phys. Rev. Lett.* **82** (1999) 4582, © 1999 by the American Physical Society.

above which center vortices are unable to confine (e.g., see Chapter 9 and Cheng et al. [32]). This, too, suggests that confinement is necessary for CSB for quarks because if there were another significant mechanism, it might show up once confinement was out of the picture.

In the picture of center vortices and nexuses supported by gluon-mass generation, it is easy to see how this happens. Center vortices give confinement, as we know, and nexuses, plus vortex twist and writhe, give topological charge and CSB. Removing center vortices takes away all these effects because nexus world lines are required to live on center vortices.

The Atiyah–Singer theorem and the Banks–Casher relation [33] (showing that CSB requires a condensate of fermionic zero modes associated by the Atiyah–Singer theorem with topological charge) say that there should be fermionic zero modes (solutions of the massless Dirac equation) localized near the topological charge produced by vortex-nexus linking. Some appropriate zero modes have been found for just such linkings [34]. Clearly, when vortices are removed in lattice simulations, such zero modes, and apparently the whole fermionic condensate, should vanish.

On the other hand, confinement is not always necessary for CSB. Dirac fermions[9] in the adjoint representation show CSB [35, 36, 37] on the lattice, and of course, the adjoint representation is not confined. Some other mechanism must be at work,

---

[9] Not Majorana fermions, so supersymmetry is not an issue. In fact, Majorana fermions are impossible in Euclidean space.

which may be well approximated by a conventional gap equation based on one-gluon Feynman graphs. The gluon is coupled to the adjoint with a strength 9/4 times its coupling to quarks, so it can happen that the gap equation breaks CSB for the adjoint but not for quarks, depending on the size of $\alpha_s(0)$ [38]. The PT estimates for $\alpha_s(0)$ are in a range where just this happens [39, 40].

It is only recently that powerful lattice algorithms for chiral quarks have come into widespread use, and so there still remains much to be done in confirming the dominant role of center vortices and nexuses in CSB for quarks. However, all present indications are favorable.

References

[1] J. M. Cornwall, Nexus solitons in the center vortex picture of QCD, *Phys. Rev.* **D58** (1998) 105028.
[2] J. Ambjorn and J. Greensite, Center disorder in the 3D Georgi-Glashow model, *JHEP* **9805** (1998) 004.
[3] M. N. Chernodub, M. I. Polikarpov, A. I. Veselov, and M. A. Zubkov, Aharonov-Bohm effect, center monopoles and center vortices in *SU*(2) lattice gluodynamics, *Nucl. Phys. B Proc. Suppl.* **73** (1999) 575.
[4] B. L. G. Bakker, A. I. Veselov, and M. A. Zubkov, The simple center projection of *SU*(2) gauge theory, *Phys. Lett.* **B497** (2001) 159.
[5] J. M. Cornwall, Dynamic problems of baryogenesis, in *Unified Symmetry: In the Small and in the Large: Proceedings of the Conference, Coral Gables, Florida, 1994*, edited by B. Kursonoglu et al. (Plenum, New York, 1994) 243.
[6] J. M. Cornwall and B. Yan, String tension and Chern-Simons fluctuations in the vortex of $d = 3$ gauge theory, *Phys. Rev.* **D53** (1996) 4638.
[7] M. Engelhardt, Center vortex model for the infrared sector of Yang-Mills theory – topological susceptibility, *Nucl. Phys.* **B585** (2000) 614.
[8] M. Engelhardt and H. Reinhardt, Center projection vortices in continuum Yang-Mills theory, *Nucl. Phys.* **B567** (2000) 249.
[9] R. Bertle, M. Engelhardt, and M. Faber, Topological susceptibility of Yang-Mills center projection vortices, *Phys. Rev.* **D64** (2001) 074504.
[10] H. Reinhardt, Topology of center vortices, *Nucl. Phys.* **B628** (2002) 133.
[11] J. M. Cornwall and G. Tiktopoulos, Three-dimensional gauge configurations and their properties in QCD, *Phys. Lett.* **B181** (1986) 353.
[12] A. M. Polyakov, Quark confinement and topology of gauge groups, *Nucl. Phys.* **B120** (1977) 429.
[13] J. M. Cornwall, Center vortices, nexuses, and the Georgi-Glashow model, *Phys. Rev.* **D59** (1999) 125015.
[14] J. M. Cornwall, Quark confinement and vortices in massive gauge-invariant QCD, *Nucl. Phys.* **B157** (1979) 392.
[15] J. M. Cornwall, A three-dimensional scalar field theory model of center vortices and its relation to *k*-string tensions, *Phys. Rev.* **D70** (2004) 065005.
[16] J. M. Cornwall, Center vortices, nexuses, and fractional topological charge, *Phys. Rev.* **D61** (2000) 085012.
[17] J. M. Cornwall, On topological charge carried by nexuses and center vortices, *Phys. Rev.* **D65** (2002) 085045.

[18] L. Kaufmann, *On Knots* (Princeton University Press, Princeton, 1987).

[19] E. Witten, Current algebra theorems for the $U(1)$ "Goldstone boson," *Nucl. Phys.* **B156** (1979) 269.

[20] G. Veneziano, $U(1)$ without instantons, *Nucl. Phys.* **B159** (1979) 213.

[21] F. R. Klinkhamer and N. S. Manton, A saddle-point solution in the Weinberg-Salam theory, *Phys. Rev.* **D30** (1984) 2212.

[22] N. S. Manton, Topology in the Weinberg-Salam theory, *Phys. Rev.* **D28** (1983) 2019.

[23] J. M. Cornwall, Semiclassical physics and confinement, in *Deeper Pathways in High-Energy Physics: Proceedings of the Conference, Coral Gables, Florida, 1977*, edited by B. Kursonoglu et al. (Plenum, New York, 1977) 683.

[24] E. V. Shuryak and T. Schafer, The QCD vacuum as an instanton liquid, *Ann. Rev. Nucl. Part. Sci.* **47** (1997) 359.

[25] K. M. Bitar and S. J. Chang, Vacuum tunneling of gauge theory in Minkowski space, *Phys. Rev.* **D17** (1978) 486.

[26] J. M. Cornwall, High temperature sphalerons, *Phys. Rev.* **D40** (1989) 4130.

[27] J. M. Cornwall and N. Graham, Sphalerons, knots, and dynamical compactification in Yang-Mills-Chern-Simons theories, *Phys. Rev.* **D66** (2002) 065012.

[28] A. Casher, Chiral symmetry breaking in quark confining theories, *Phys. Lett.* **83B** (1979) 395.

[29] J. F. Donoghue and K. Johnson, The pion and an improved static bag model, *Phys. Rev.* **D21** (1980) 1975.

[30] J. M. Cornwall, Confinement and chiral symmetry breakdown: Estimates of F_π and of effective quark masses, *Phys. Rev.* **D22** (1980) 1452.

[31] P. de Forcrand and M. D'Elia, Relevance of center vortices to QCD, *Phys. Rev. Lett.* **82** (1999) 4582.

[32] M. Cheng et al., Transition temperature in QCD, *Phys. Rev.* **D74** (2006) 054507.

[33] T. Banks and A. Casher, Chiral symmetry breaking in confining theories, *Nucl. Phys.* **B169** (1980) 103.

[34] H. Reinhardt, O. Schroeder, T. Tok, and V. C. Zhukovsky, Quark zero modes in intersecting center vortex gauge fields, *Phys. Rev.* **D66** (2002) 085004.

[35] J. Engels, S. Holtmann, and T. Schulze, The chiral transition of $N_f = 2$ QCD with fundamental and adjoint fermions, *PoS* **LAT2005** (2006) 148.

[36] F. Basile, A. Pelissetto, and E. Vicari, The finite-temperature chiral transition in QCD with adjoint fermions, *JHEP* **0502** (2005) 044.

[37] F. Karsch and M. Lutgemeier, Deconfinement and chiral symmetry restoration in an $SU(3)$ gauge theory with adjoint fermions, *Nucl. Phys.* **B550** (1999) 449.

[38] J. M. Cornwall, Center vortices, the functional Schrödinger equation, and CSB, arXiv 0812.1870 [hep-ph].

[39] A. C. Aguilar, D. Binosi, and J. Papavassiliou, Infrared finite effective charge of QCD, *PoS* **LC2008** (2008) 050.

[40] A. C. Aguilar, D. Binosi, J. Papavassiliou, and J. Rodriguez-Quintero, Non-perturbative comparison of QCD effective charges, *Phys. Rev.* **D80** (2009) 085018.